STRUCTURAL MODELLING OF MULTILAYER SKIS WITH AN OPEN SOURCE FEM SOFTWARE

LORENZO FRACCAROLI[1], CARLO GORLA[2] & FRANCO CONCLI[1]
[1]Faculty of Science and Technology, Free University of Bolzano/Bozen, Italy
[2]Politecnico di Milano, Italy

ABSTRACT

The design process of a ski is characterized by a short time of development due to continuous advancements in the material science and in the manufacturing processes as well as in customer's requirements. Nowadays, the development process is very often still based on several physical prototypes and trials and Finite Elements Analysis (FEA) is a significant method to reduce times needed. The aim of this work is to develop a reliable numerical simulation of an existing mountaineering ski, able to predict the performance of the real element. For this purpose, an initial mechanical characterization of all the constituents used in the ski manufacturing was performed. Tensile tests in two directions were performed on flat bone-shaped samples laser cut from sheets. Combining the results of the tensile tests with Digital Image Correlation (DIC) data it was possible to approximate the four in-plane (XY) elastic properties, namely, the two elastic modules, the shear module and the Poisson ratio (E_x, E_y, G_{xy}, ν_{xy}). The DIC free software used is GOM Correlate. Results of the combined "tensile tests – DIC" approach were after verified with FEM simulations reproducing the testing configuration. The digital model of the ski was created starting from the nominal geometry. The whole procedure of modelling, meshing and FE analysis was performed in the open source software Code_Aster/Salome-Meca. Using this kind of software, which code is free to use and modify, permits to reduce costs due to its free license. The real component was tested in a three-point bending and torsion test. This kind of experiments were replicated on the FEM model and results were compared. The comparison highlighted discrepancies of 2.5%–10% with respect to the real component.
Keywords: ski mountaineering, FEM, Code_Aster, DIC, composite materials, Salome-Meca.

1 INTRODUCTION

The current approach to the design of ski-mountaineering (skimo or skialp), and of those designed for racing purposes, is characterized by a relevant testing activity. Typically, several prototypes are manufactured, and a preliminary screening is based on the based on the experimental measurement of their basic mechanical properties, like torsional and bending behavior. After that, best prototypes are tested by professionals, who can give feedback on feelings and behaviors of the ski in real conditions. Even if, especially in the case of small companies, the prototyping process is very often quite efficient, it is evident that this trial and error procedure has significant disadvantages like the cost for manufacturing prototypes and the time needed for manufacturing and testing the sport equipment. The chance of reducing the necessary physical prototypes, based on a preliminary overview by means of virtual prototypes could represent an improvement of the whole design and manufacturing process. Simulations based on the use numerical techniques such Finite Element Analysis (FEA) represent a suitable solution for the scope under discussion. These numerical techniques have been used for the design phases of race-carving skis [1]–[4]. The mechanical properties and behavior of downhill component is highlighted in [5]–[7], however, the FEA approach is not yet used for development in the skimo sector. In this particular snow-sport it is very important to find a compromise between weight and in-operation behavior, this fact increases the difficulty during design phase of the component.

The objective of this research was to develop a numerical model of a mountaineering ski based on data corresponding to a model already on the market produced by a leader

WIT Transactions on Engineering Sciences, Vol 133, © 2021 WIT Press
www.witpress.com, ISSN 1743-3533 (on-line)
doi:10.2495/MC210031

manufacturing company. The real skis have been subjected to experimental bending tests as well as specimens of the different materials used in the ski manufacturing process. A preliminary material characterization phase took place. Classic dog bone shape specimens were produced thanks to laser cut technology. It has to be pointed out that the test procedures are not necessarily based on the standard methods defined for each class of materials because the aim of the tests was to determine the mechanical properties to be introduced in the models and not prepare a complete technical datasheet of the material. Specimens created from material sheets were tested (tensile test) in the two principal directions. In exception for some materials in which only one test in each direction was done (due to low constituents' availability), two tests were performed in each direction. In order to characterize materials the use of Digital Image Correlation (DIC) [8]–[15] and Campbell [16] hypothesis was mandatory. During the development of the numerical model different simplifications were introduced. To conclude, real tests results (torsion and bending) [15], [17] were compared with the one achieved with the FEM simulation.

2 MATERIALS AND METHODS

2.1 Ski overview

Skis are usually produced with a composite structure that foresees different layers. The core of the component is typically made by a very lightweight and flexible material like wood or honeycomb. The inner part is protected with multilayer constituents like carbon, basalt and glass fibers reinforced materials. These reinforcement components play the major role for the resistance and stiffness of the ski. Moreover, the ski includes materials not having structural purposes, like the lower and the top layer. These are used for other reasons: the upper part is for improving the quality of the decoration of the ski while the lower material is chosen in order to reduce the friction of the ski on the snow. It is evident that it is fundamental to find a balance between all constituents in order to reach the best configuration with respect of the performances of the ski. This objective is even more difficult to fulfil when the weight reduction is fundamental, as for the racing skies or for skies which are aimed at a high market level, in which a lightweight design must be obtained without affecting the downhill performances. In such conditions, solutions with an increased number of layers represent the most suitable solutions: it is evident that without the use of numerical simulations like FEA the development time increases hugely, moreover the knowledge of the manufacturer represent the unique available tool.

2.2 Material characterization

Since material properties were not known, the first phase of the research was dedicated to the characterization of mechanical properties of each constituent present in the real component. Skies considered are built up with different layers of composites materials with a central wood softcore. Composites materials have two major constituents, fibers and matrix. Fibers take a major part of the load during operation while matrix must keep fibers together and protect them from external agents. For describing the mechanical behaviour of composites materials, the theory of orthotropic laminas and laminated structures has been used. The material was considered having just one principal direction. Orthotropic materials can be described in 3D by means of nine independent elastic constants, compared with the 21 required for a completely non isotropic material. For thin laminas that has only continuous fibers, behaviour can be described with four independent elastic constants: the two elastic

modules, the in-plane shear module and one of the two in-plane Poisson's ratios. In this research, the two elastic modules were obtained directly from unidirectional tensile tests and the Poisson's ratio was extrapolated from Digital Image Correlation (DIC) measurements. The shear module was estimated with the approximated Campbell equation [16].

Materials are recognized by means of a code number. Specifically, 9, 24, 139, 207, 290, 135, 31, 86 and 217. Monoaxial tests were performed on an STEPLab UD04 (Fig. 1) testing machine capable to apply static forces up to 4.5 kN. Tests crosshead speed was set at 0.1 mm/min. While the elastic modules can be directly obtained from the tensile tests, the estimation of the Poisson's ratio requires the calculation of the strains in two directions (eqn (1))

$$\nu_{xy} = -\frac{\varepsilon_y}{\varepsilon_x} \; ; \; \nu_{yx} = -\frac{\varepsilon_x}{\varepsilon_y}. \tag{1}$$

One option could be the adoption of multiaxial strain gauges. However, Digital Image Correlation (DIC) represents a valid alternative. One camera (reflex Nikon D750 with a 24–85 zoom and a stabilizer), acquires pictures during timestep. A correct illumination was guaranty by a dedicated lamp source.

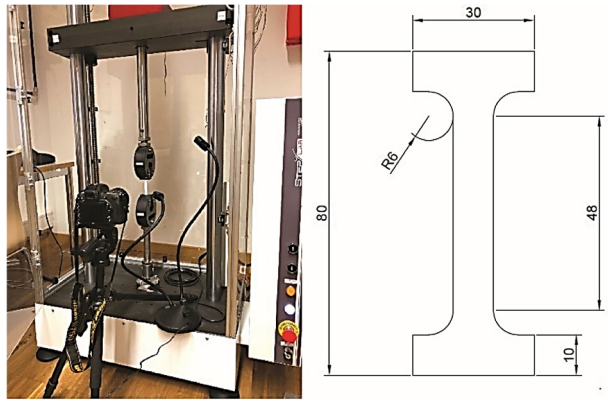

Figure 1: STEPLab UD04 tensile machine and testing setup; (right) dog-bone sample geometry and dimensions.

2D Digital Image Correlation is an advanced optical measurement technique that allows to reconstruct displacement and strain fields of an inspected component having a planar surface. This technology is based on the greyscale; therefore, a characteristic "speckle" pattern based on the gray scale must be made on the inspected surface before testing. The camera should be positioned perpendicularly to the specimen surface in order to avoid out of plane measurements. The camera acquired image during the tensile test with a constant time step. The first picture acquired (undeformed sample) is used as reference. The post-processing algorithm creates a virtual grid on the image of the specimen's surface dividing the total area into several smallest areas called subsets or facets. Cross correlation operations allow the recognition of facets during each step (equivalent to diverse picture and displacements) (Fig. 2). When all facets are recognized at each time, the algorithm reconstructs the displacement field and successively the strain field of the tested component. The package used is GOMrrelate [18].

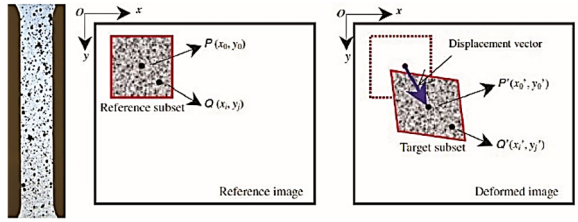

Figure 2: DIC; (left) surface pattern; (right) cross correlation.

In this manner it is possible to measure strains in the two different directions. With these new data is now possible to calculate the Poisson ratio with (eqn (1)), while the shear module is computed with the Campbell equation (eqn (2))

$$G_{xy} = \frac{E_x}{(1+\nu_{xy})} + \frac{E_y}{(1+\nu_{yx})}. \tag{2}$$

2.3 FEA

In this work the open source computer software Code_Aster/Salome-Meca was used. It is an open source Finite Element (FE) environment developed by EDF (Électricité de France). In Fig. 3 is visible the load configuration of the tested ski.

Two reproductions with different levels of simplifications were tested.

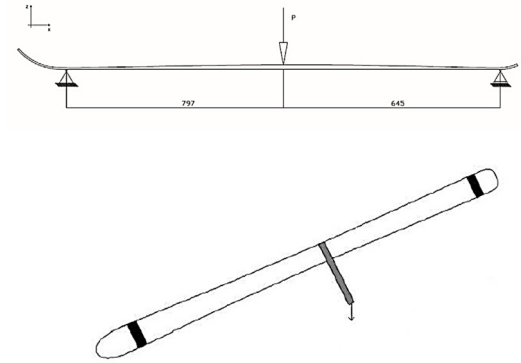

Figure 3: Load configuration: the three-point bending (up) and torsion-bending tests (bottom) – reference case for the FE simulations.

2.3.1 Shell-model

Considering the configuration of the three-point bending test, some geometrical considerations were made. First, it was decided to exploit the z–x plane symmetry of the ski, therefore only one half of the structure was modeled. Secondly, tail and top were cut off in order to consider only the component that lay between supports. In addition, also steel laminas were neglected due to their very low structural contribution. Fig. 4 shows the shell model. All the small subdivision that can be seen were necessary for correctly defining the

height of the ski. The shell modelling in Code_Aster/Salome-Meca does not recognize curved surfaces, therefore at each small area was assigned the correspondent value of thickness. The component was separated into 145 parts in order to have a better estimate of the curvature of the component. The final grid consists in 22,382 quadrangular mesh elements. The torsion-bending test was simulated numerically with a similar model, without exploiting the z–x plane-symmetry.

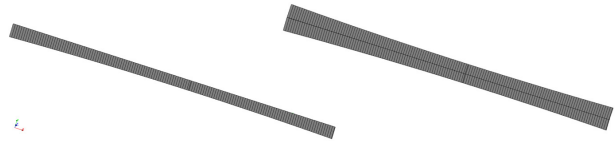

Figure 4: Shell models used for the three-point-bending (left) and torsion-bending (right) simulations.

2.3.2 Solid-model

The 3D modelling foresees to exploit the same simplifications used for the 2D analysis. The same geometrical simplifications of the shell-model were used also for the 3D simulations. Moreover, other simplifications were necessary for defining correctly material parameters. As explained in Section 2.1, for describing composites material in the three-dimensional case are necessary nine elastic constants. According to Aerospaziali [19], if materials are composed by only unidirectional long fibers, it is possible to assume that elastic modules in the radial direction are the same. Moreover, tests were done on low thickness laminas, this fact does not permit to follow standards for computing the outstanding out of plane properties. For this reason, Module G and Poisson's ratio were set equal to the one obtained previously with the in-plane (eqn (1)) and (eqn (2)) considerations. Assumptions taken were the following: Poisson's ratios and shear modules were set equal in each of the three principal directions while the third elastic module was set equal to the one in the y direction. On the other hand, as shown in Figs 5 and 6, in the solid model the lateral protective layer was also considered.

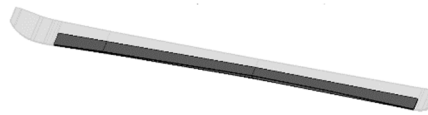

Figure 5: Isometric view of the solid model used for the three-point-bending test.

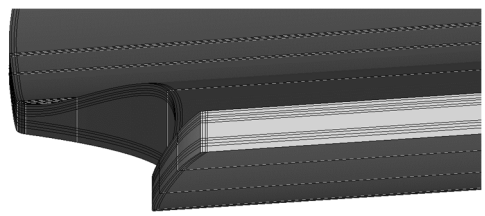

Figure 6: Different layers of the solid model.

Three finite elements in the thickness were created for each material layer to correctly describe the stress profile. The grid was formed by quadratic hexahedrons. A total mesh of 500 k cells was created for the three points bending model.

3 RESULTS

The results of the tensile test in terms of stress strain curves and numerical values are presented in Figs 7–13 and Table 1 respectively.

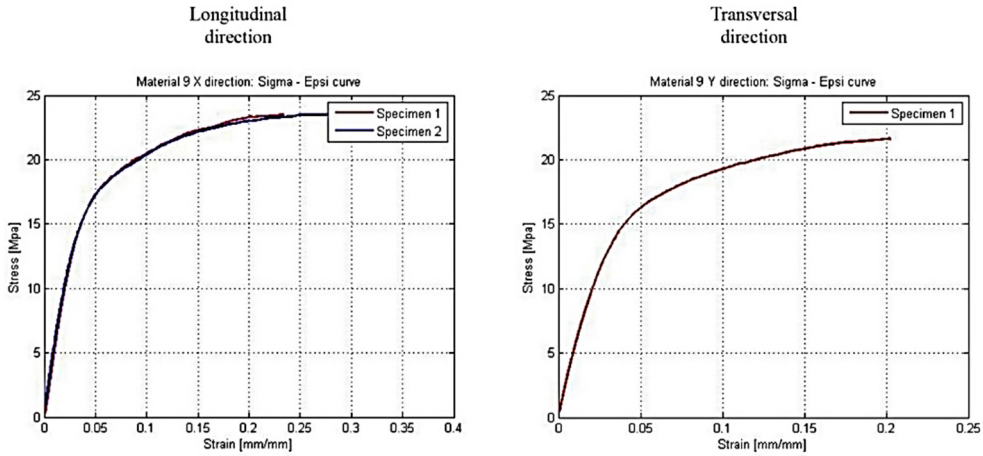

Figure 7: Material 9 tensile tests.

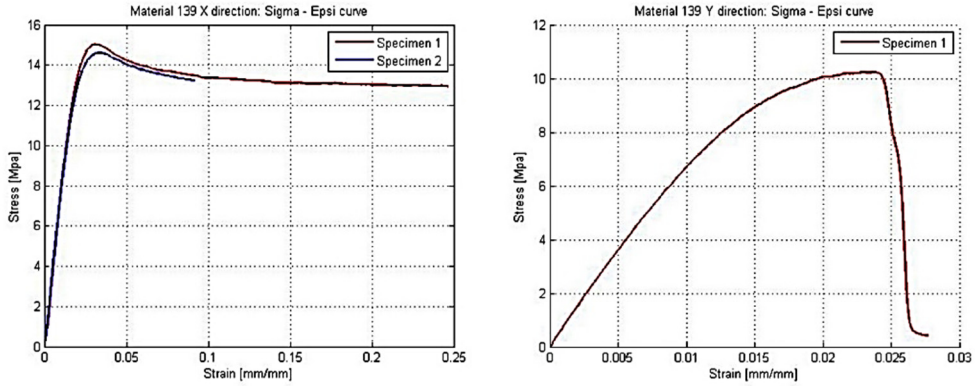

Figure 8: Material 139 tensile tests.

Table 2 shows the higher displacement of the center of the ski when subjected to a load of 120 N in the three-point bending tests. Tests were performed with the help of two supports and a kettlebell for applying the load. Ski was blocked to the supports thanks to two clamps and the kettlebell positioned on the ski through its handle. Results for both experimental and numerical approach were confronted. Table 3 reports the results of the torsion-bending tests and simulations.

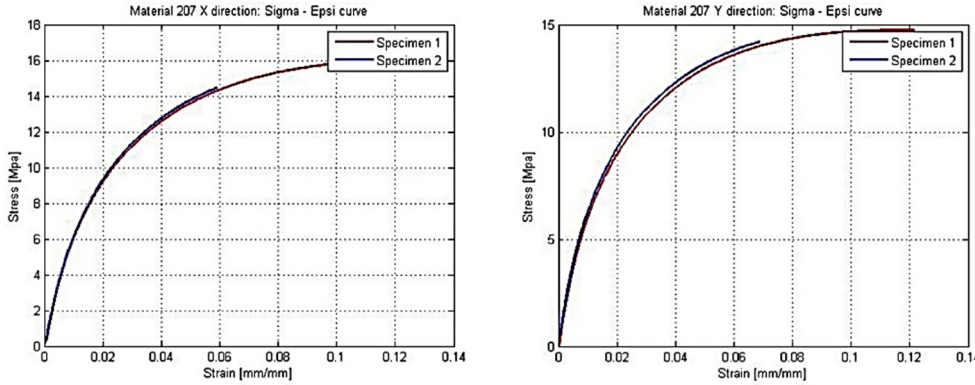

Figure 9: Material 207 tensile tests.

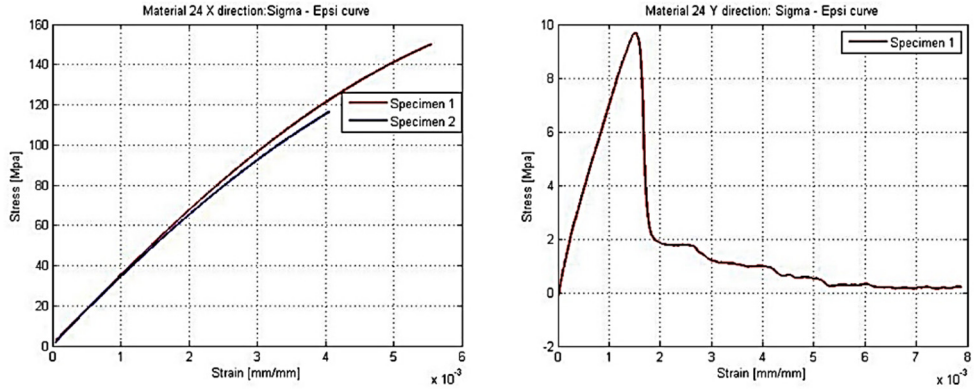

Figure 10: Material 24 tensile tests.

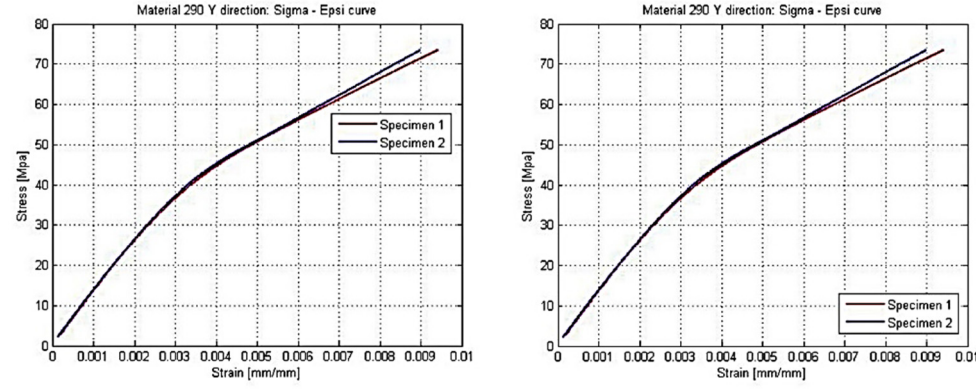

Figure 11: Material 290 tensile tests.

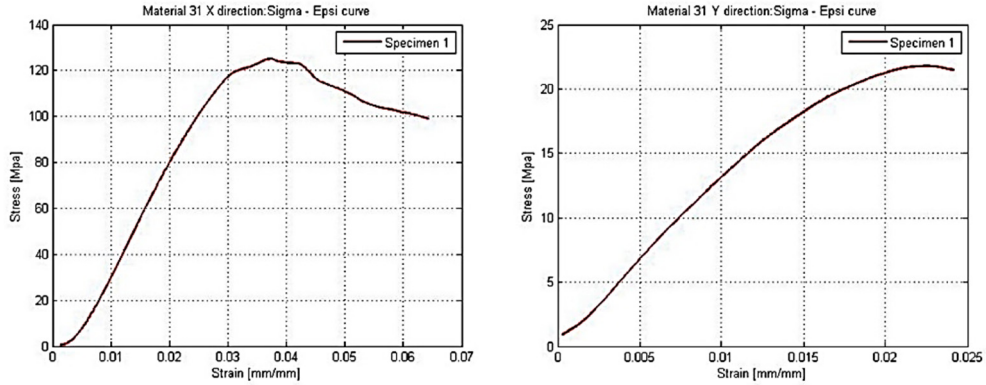

Figure 12: Material 31 tensile tests.

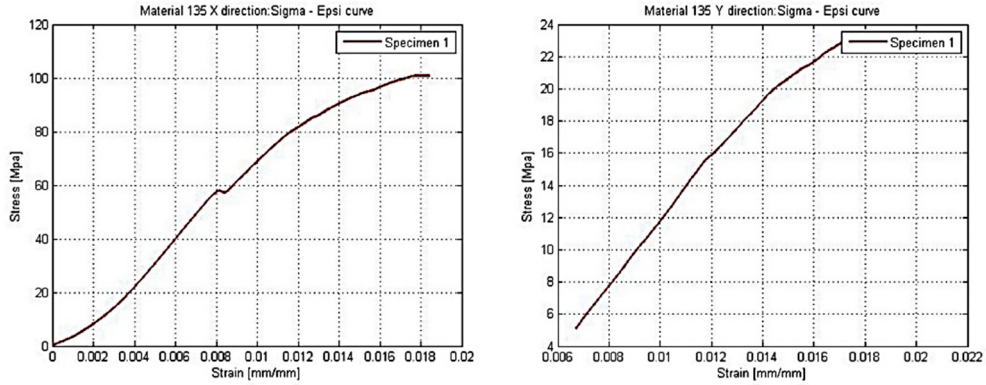

Figure 13: Material 135 tensile tests.

Table 1: In-plane properties of the tested materials.

	Material								
Material #	9	24	139	207	290	135	31	86	217
E_x (MPa)	550	35,000	800	850	20,000	4,000	2,000	13,700	35,000
E_y (MPa)	567	8,700	750	897	13,700	569	127	420	12,436
ν_{xy} (-)	0.45	0.23	0.45	0.42	0.18	0.39	0.39	0.40	0.56
ν_{yx} (-)	0.43	0.35	0.38	0.30	0.12	0.39	0.39	0.40	0.48
G_{xy} (MPa)	776	35,010	1,097	1,291	29,125	3,009	1,184	10,086	25,327

Table 2: Comparison of the maximum deflection of the ski in the three-point bending test: FEM vs. experiments.

Model	Displacement (mm)	Simulation time* (min)	Error (%)
Experimental	40		
Shell	41	35	2.5%
Solid	44	60	10.0%
*on a 9.6 GFLOPS workstation			

Table 3: Comparison of the maximum deflection of the ski in the torsion-bending test: FEM vs. experiments.

Model	Rotation angle (°)	Simulation time* (min)	Error (%)
Experimental	4.44		
Shell	4.61	35	3.0%
Solid	4.86	60	9.5%
*on a 9.6 GFLOPS workstation			

Fig. 14 reports the normal stresses in the point in which load was applied with respect to the thickness of the ski (0 match with the lower part) during the bending test. Fig. 15 is similar but refers to the bending-torsion test.

4 DISCUSSION

Considering the nature of the ski, only the linear part of the constitutive law is of interest. Most of the tested materials does not present discrepancies in elastic field. For material #9 #24 and #139, it can be appreciated that the two repetitions in the X direction do not show differences in the linear part. In the Y direction, because off the low presence of constituents, only one probe was tested. Considering materials #207 and #290 it is possible to observe that, in both directions, no differences are present into the elastic field between the different repetitions. For materials #135 and #31 a different approach was used. In these particular

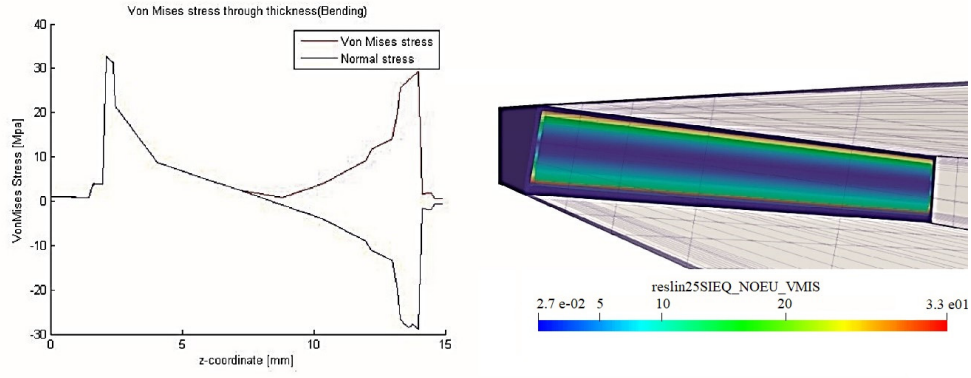

Figure 14: Solid model results – three-point-bending test (normal and Von Mises stresses in the section).

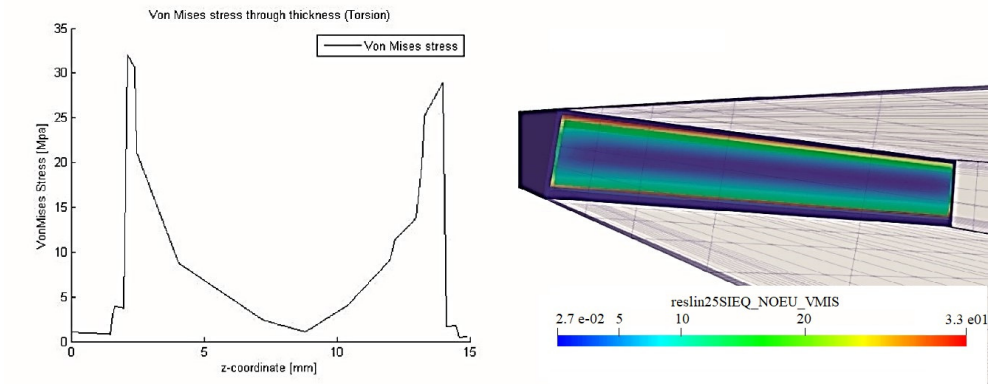

Figure 15: Solid model results – torsion-bending test (normal and Von Mises stresses in the section).

specimens it was impossible to create the classic dog bone probe, therefore a rectangular tester was obtained cutting the initial sheet of material. For these constituents, since the fibres were easily identifiable, the thickness and width of single filaments were measured. Consequently, the resistant area was obtained by multiplying the single fibres area by the total number of filaments present in the tested probe. The tests on the single material will be object of further refinement, but in this phase of the research, which is more focused on the definition of FEM models than on the exact characterization of the materials, the data collected seem enough.

FEM results shows a good agreement with the experimental measurements for both the modelling approaches (2D and 3D). The 2D analysis highlighted a maximum displacement (three-point-bending) of 41 mm with a 2.5% difference with respect to the experimental measure while the solid analysis gave as results equal to 44 mm (10% difference vs. experiments). In the torsion-bending analysis, the shell model predicts a rotation of 4.60° while the solid model a rotation of 4.86. The error with respect to the experimental measure is equal to 3% and 9.5% respectively. For the shell model, discrepancies in the predicted displacement/rotation with respect to the measured one can be attributed to the following reasons:

- Component was divided in small areas in which were assigned different values of heights, therefore the curvature of the ski is approximated and not correctly replicated.
- The steel edges and the lateral layers (cage) were neglected.

On the other side, comparing the solid model with the experimental test, it is possible to give some motivation for the higher discrepancy including:

- The ski was considered straight without considering its shape in the longitudinal direction.
- Simplification introduced during the material characterization phase may affect results

Differences between the solid model and the shell one is also due to the lateral cage. Both configurations have equal width, but the cage were simulated only in the 3D approach. Bending contribution of these lateral constituents component is lower with respect to the main core part of the ski. From Figs 14 and 15 it can be appreciated that some constituents

do not give resistant contribution. This fact is highlighted considering materials at the border of the ski (bottom and top layer). Although their displacement, it is possible to see that they are not loaded. In fact, their contribution is for example to reduce the friction with the ground (bottom layer) or improve the insulation of the component form external agents that may degrade the internal layers. FEA allows an accurate evaluation on how each layer is contributing to the total stiffness of the ski.

These considerations are valid for both models (Three-point bending and torsion-bending tests). However, for the last mentioned it is possible to give a further consideration for explaining results discrepancies. Generally, for torsion the shear module G plays a pivotal role, it is possible that the fact that it was approximated and not directly computed may influenced results.

5 CONCLUSIONS

An accurate mathematical description of a real ski is still difficult to achieve. However, in this work a 2.5%–10% error approximation was reached. The difficulty to describe properly materials that were composing the sandwich structure influenced hugely the model replication. The fact that materials dimensions do not permit to follow standards has to be considered when evaluating results. The elastic module was calculated for each constituent (For material #86 and #217 properties are available in literature). Considering the results of the final simulations, it is possible to achieve satisfactory levels of approximation. The use of DIC was mandatory for a complete material characterization. The comparison between the real model and FEM simulations of three-point bending and torsion-bending tests was made. Better results were obtained with the shell approach. The solid model has a higher percentage error due to material parameters simplifications. However, theoretical predictions of the stress state and the behavior of the ski when subjected under bending were confirmed by experimental test. For the torsion-bending shell model, a maximum error of the 3% was found while for the solid one a 9.5% discrepancy was recorded. As for the bending case the plane model presents more reliable results. This fact is due to the lower level of approximation used in the 2D problem.

Once the model is validated it will be possible to easily change materials properties and layers dimensions having a virtual comparison between different design solutions. This fact can lead to a reduction of the time needed for ski development. Moreover, the need to produce several physical prototypes is not more necessary, as consequence it will be possible to decrease research and development costs. Future improvements will be a more accurate modelling of the ski without simplification in terms of material properties. The fact that steel edges were not modelled, influenced securely the performance of the ski.

It must be pointed out that in the real application the effective load conditions on the ski are much more complex and difficult to determine. The loads are applied in all the directions and the reaction coming from the contact with the snow are variable and strongly affected by the deflections of the ski and by the deformation of the snow. Moreover, the behaviour of the snow itself is widely variable and influenced by many parameters (temperature, humidity, time from the deposition, thermal and mechanical cycles experienced, etc.).

For this reason the validation of the simulation of ski under real load condition represents a hard job and also models of the snow should be considered, validated experimentally compared with simulations in a FE environment in order to verify the accuracy of the FEM ski model. These issues will be investigated in the next steps of the research. In conclusion it should be highlighted that while the results achieved are not perfectly reproducing the real ski performance, the accuracy is satisfactory considering all the simplifications and hypothesis introduced.

REFERENCES

[1] Wolfsperger, F., Szabo, D. & Rhyner, H., "Development of alpine skis using FE Simulations," *Procedia Eng*., **147**, pp. 366–371, 2016. DOI: 10.1016/j.proeng.2016.06.314.

[2] Federolf, P., Roos, M., Lüthi, A. & Dual, J., Finite element simulation of the ski-snow interaction of an alpine ski in a carved turn. *Sport. Eng*., **12**(3), pp. 123–133, 2010. DOI: 10.1007/s12283-010-0038-z.

[3] Zboncak, R., Experimental verification of ski model for finite element analysis. *Conf. Experimental Stress Anal.*, **56,** pp. 450–456, 2018.

[4] Mössner, M., Innerhofer, G., Schindelwig, K., Kaps, P., Schretter, H. & Nachbauer, W., Measurement of mechanical properties of snow for simulation of skiing. *J. Glaciol*., **59**(218), pp. 1170–1178, 2013. DOI: 10.3189/2013JoG13J031.

[5] Nordt, AAGSSLPK, Computing the mechanical properties of alpine skis. *Sport. Eng*., **2**(2), p. 65, 1999. DOI: 10.1046/j.1460-2687.1999.00026.x.

[6] Hirano, Y. & Tada, N., Mechanics of a turning snow ski. *Int. J. Mech. Sci*., **36**(5), pp. 421–429, 1994. DOI: 10.1016/0020-7403(94)90045-0.

[7] Cresseri, S. & Jommi, C., Snow as an elastic viscoplastic bonded continuum: A modelling approach. *Ital. Geotech*., **4**, pp. 43–58, 2005.

[8] Musotto, Z., Digital Image Correlation : Correlation applicazione di tecniche convenzionali e sviluppo di soluzioni la stima e l ' incremento dell ' accuratezza, 2012.

[9] Crammond, G., Boyd, S.W. & Dulieu-Barton, J.M., Speckle pattern quality assessment for digital image correlation. *Opt. Lasers Eng*., **51**(12), pp. 1368–1378, 2013. DOI: 10.1016/j.optlaseng.2013.03.014.

[10] Makeev, A., He, Y., Carpentier, P. & Shonkwiler, B., A method for measurement of multiple constitutive properties for composite materials. *Compos. Part A Appl. Sci. Manuf*., **43**(12), pp. 2199–2210, 2012. DOI: 10.1016/j.compositesa.2012.07.021.

[11] Kowalczyk, P., Identification of mechanical parameters of composites in tensile tests using mixed numerical-experimental method. *Meas. J. Int. Meas. Confed*., **135**, pp. 131–137, 2019. DOI: 10.1016/j.measurement.2018.11.027.

[12] Schreier, H.W. & Sutton, M.A., Systematic errors in digital image correlation due to undermatched subset shape functions, pp. 303–310.

[13] Wattrisse, B., Chrysochoos, A. & Muracciole, J., Analysis of strain localization during tensile tests by digital image correlation. pp. 29–39, 2000.

[14] Peters, W.H. and Ranson, W.F., Digital image techniques in experimental stress analysis. *Opt. Eng*., **21**(3), pp. 427–431, 1982.

[15] Górszczyk, J., Malicki, K. & Zych, T., Application of digital image correlation (DIC) method for road material testing. *Materials (Basel)*, **12**(15), p. 2349, 2019. DOI: 10.3390/ma12152349.

[16] Yokoyama, T. & Nakai, K., Evaluation of in-plane orthotopic elastic constants of paper and paperboard. *Proc. SEM Annu. Conf. Expo. Exp. Appl. Mech*, **3**(2007), pp. 1505–1511, 2007.

[17] Fraccaroli, L. & Concli, F., Introduction of open-source engineering tools for the structural modeling of a multilayer mountaineering Ski under operation. *Appl. Sci.*, **10**(15), 2020.

[18] www.gom.com.

[19] Aerospaziali, T.E.M., CAPITOLO 32 - materiali compositi: la legge costitutiva ortotropa.